Journal of Applied Physics ARTICLE scitation.org/journal/jap

Formation of carbon interstitial-related defect levels by thermal injection of carbon into *n*-type 4*H*-SiC

Cite as: J. Appl. Phys. **131**, 035702 (2022); doi: 10.1063/5.0077308
Submitted: 1 November 2021 · Accepted: 28 December 2021 ·
Published Online: 18 January 2022

View Online Export Citation CrossMark

Robert Karsthof,[1,a)] Marianne Etzelmüller Bathen,[1,2,3] Andrej Kuznetsov,[3] and Lasse Vines[3]

AFFILIATIONS

[1]Centre for Materials Science and Nanotechnology, University of Oslo, 0316 Oslo, Norway
[2]Advanced Power Semiconductor Laboratory, ETH Zürich, Physikstrasse 3, 8092 Zürich, Switzerland
[3]Department of Physics, University of Oslo, 0316 Oslo, Norway

Note: This paper is part of the Special Topic on Defects in Semiconductors.
[a)]**Author to whom correspondence should be addressed:** r.m.karsthof@smn.uio.no

ABSTRACT

Electrical properties of point defects in 4*H*-SiC have been studied extensively, but those related to carbon interstitials (C_i) have remained elusive until now. Indeed, when introduced via ion irradiation or implantation, signatures related to C_i observed by deep level transient spectroscopy tend to overlap with those of other primary defects, making the direct identification of C_i-related levels difficult. Recent literature has suggested to assign the so-called M center, often found in as-irradiated 4*H*-SiC, to charge state transitions of the C_i defect in different configurations. In this work, we have introduced excess carbon into low-doped *n*-type 150 μm thick 4*H*-SiC epilayers by thermal annealing, with a pyrolyzed carbon cap on the sample surface acting as a carbon source. Because the layers exhibited initially low concentrations of carbon vacancies ($[V_C] = 10^{11}$cm), this enabled us to study the case of complete V_C annihilation and formation of defects due to excess carbon, i.e., carbon interstitials C_i and their higher-order complexes. We report on the occurrence of several new levels upon C injection, which are likely C_i-related. Their properties are different from those found for the M center, which point toward a different microscopic identity of the detected levels. This suggests the existence of a rich variety of C_i-related defects. The study will also help generating new insights into the microscopic process of V_C annihilation during carbon injection processes.

Published under an exclusive license by AIP Publishing. https://doi.org/10.1063/5.0077308

I. INTRODUCTION

Point defects in the 4*H* polytype of silicon carbide (4*H*-SiC) exhibit great technological potential in novel quantum technologies; on the other hand, such defects can have detrimental effects on power device operation. Specifically, the silicon vacancy (V_{Si}) and related complexes can be functionalized for single-photon emission and coherent spin manipulation.[1–4] Meanwhile, the carbon vacancy (V_C) is notorious for limiting the minority carrier lifetime[5] and having a detrimental impact on the performance of bipolar power devices. However, despite extensive studies on the fundamental defects and their complexes in 4*H*-SiC, the electrical signatures of interstitial defects remain elusive.

Deep level transient spectroscopy (DLTS) spectra of as-grown n-type 4*H*-SiC commonly exhibit the ever-present $Z_{1/2}$ and $EH_{6/7}$ levels, which were assigned to the (0/2−) and the deeper-lying (2+/+/0) charge transition levels of the carbon vacancy, respectively.[6,7] Upon irradiation, other defect levels appear, including the EH_4 and EH_5 levels[8,9] (recently tentatively assigned to the carbon antisite-vacancy pair[10]), the S center[11] (attributed to the Si vacancy[12]), $EH_{1/3}$,[13,14] and the M center.[15–18] Intriguingly, the latter three defect levels (S_1/S_2, EH_1/EH_3, and M_1/M_3) are reported in the same regions of the DLTS spectra and often overlap. The M center is metastable,[15,17] while $EH_{1/3}$ has been found to arise after electron irradiation below the assumed silicon displacement limit.[14] Depending on the study, different formation and annealing parameters are reported, and some controversy remains regarding the assignment and nomenclature of the different defect species. It was noted that the photoluminescence emission intensity from defects in 4*H*-SiC, e.g., from the V_{Si}, is enhanced after annealing at

Published under an exclusive license by AIP Publishing

100–600 °C depending on the implantation species.[19] This has been partly ascribed to the annealing of C_i, as it is expected to be an efficient non-radiative recombination center, reducing the overall luminescence irradiated samples.

C_i was predicted to be electrically active early on.[20–22] Direct identification has proven challenging, but C_i may account for instabilities that arise in the DLTS spectra of n-type 4*H*-SiC immediately after irradiation but disappear upon heat treatments at 100–300 °C.[10,23] A recent study on He-implanted 4*H*-SiC, combining DLTS measurements and density functional theory calculations, aimed to address C_i directly by assigning the M center to the carbon self-interstitial.[24] The bistability was attributed to conversion between C_i at the hexagonal (*h*) and pseudo-cubic (*k*) lattice sites. However, the unavoidable presence of vacancy-related defects after irradiation prevents the study of interstitial-related defects in an unobstructed environment.

The involvement of C_i has been discussed extensively in the context of V_C control. The V_C is perennially present in state of the art 4*H*-SiC epitaxial layers,[25] and its presence has been correlated to lower minority carrier lifetimes[5] having a negative impact on bipolar device operation. Removal of the V_C is thus of strong interest, and three main strategies have been devised: (i) near-surface implantation of ions and subsequent annealing leading to V_C annihilation,[26–29] (ii) thermal oxidation of the epilayer surface, promoting injection of Si and C into the bulk material,[28,30,31] and (iii) thermal equilibration of V_C by annealing in the presence of a carbon cap.[32,33] Common to all three methods is the presence of an excess of mobile atom species moving through interstitial lattice sites, promoting the disappearance of V_C by the atoms occupying V_C sites. In this regard, carbon appeals as the most suitable diffusing species since it completely annihilates with V_C without introducing new defect levels. While the methods (i)–(iii) have been shown to work well, the introduction and migration through the 4*H*-SiC lattice is not well understood because the amount of excess carbon is usually lower than the concentration of V_C defects. It is sometimes assumed that diffusion of C mono-interstitials (C_i) dominates; however, C_i is also known to be an unstable defect that often binds to other defect species or to form carbon complexes. Therefore, the question arises whether instead, C diffusion is mediated by higher-order carbon complexes. To directly observe C_i-related defect levels, epilayers with initially low [V_C] are required such that after C injection and V_C annihilation, a surplus of C_i-related defects remains.

In this study, we monitor the thermally induced introduction of excess carbon into 4*H*-SiC epi-layers in the near absence of vacancy-related defects. Excess carbon is introduced into high-purity and low-doped *n*-type 4*H*-SiC by thermal annealing using a pyrolyzed carbon cap on the sample surface acting as a C source. The low concentration of other defects prior to and during annealing enables the separation of interstitial- and vacancy-related defect levels. Additionally, the interaction between V_C and C_i is discussed where we report on several levels appearing upon C injection, with a microscopic identity of the detected levels that appears to be different from that of the M center.

II. METHODS

The studied 4*H*-SiC samples consisted of 150 μm thick epilayers doped with N ($n \approx 10^{14}$cm^{-3} as determined by capacitance–voltage measurements) grown on highly doped *c*-oriented 2″ substrates, purchased from Ascatron AB, Sweden. The samples were laser-cut into pieces of 7×7 mm^2, cleaned using the full standard RCA procedure, and then coated with photoresist (type AR-U 4030) on the sample front and backside in several spin-coating cycles (total resist thickness ≈5 μm). The coated samples were then heat-treated in an RTP furnace at a temperature of 900 °C for 10 min in vacuum ($p = 5 \times 10^{-5}$mbar) during which the photoresist was graphitized. The C-capped samples were then annealed in a tube furnace under Ar atmosphere at 1250 °C for 1.5, 2.5, and 6.6 h. It should be noted that after the high-temperature anneals, the C-cap on the samples had been almost completely dissolved, and the samples' surfaces had been oxidized to form SiO_2 (as determined using energy-dispersive x-ray spectroscopy). We attribute this to the presence of residual oxygen during the annealing process, likely due to continued outgassing of the furnace tube. It is unknown how long into the annealing the C-caps were still intact to provide a source of C. However, thermal oxidation of SiC is another common procedure to inject C into the epilayer; therefore, we believe the effect of unintended oxidation to be negligible for the interpretation of this experiment.

After annealing, the samples were RCA-cleaned, and 150 nm thick Ni Schottky contacts were deposited on the epilayer using e-beam evaporation through a shadow mask (diode area 7.85×10^{-3} cm^2). Silver paste was used as a back contact to the conductive substrate. We note that the oxidation of the epilayer surface during the annealing did not lead to a significant surface roughening or to degradation of the Schottky diode quality.

The electrical characterization (CV) was carried out using a Boonton-7200 high-precision capacitance meter, operating at a test frequency of 1 MHz. The same device, in combination with an Agilent 81110A pulse generator, was used for DLTS measurements. If not stated otherwise, the DLTS measurements were performed at a reverse bias of −20 V and pulse voltages of 20 V, using a pulse length of 50 ms, and in a temperature range between 20 and 300 K, where cooling was achieved with a closed-cycle He refrigerator. During the DLTS runs, the temperature was typically ramped with a rate of 1 K min^{-1}, starting at low temperatures and going to 300 K, during which transients of 640 ms length were continuously recorded, averaged over an interval of 0.5 K, and then mapped to the central temperature of the respective interval. The DLTS signal was then calculated on the averaged transient for each temperature. DLTS evaluation was performed using a lock-in ("GS2") and a high-resolution ("GS4") correlation function,[34,35] with six (GS4: five) rate windows between 20 ms (GS4: 40) and 640 ms.

The extraction of trap parameters, such as activation energy, capture cross section, and concentration, was in some cases achieved by simulating the DLTS spectra using the method and software described in Ref. 36.

III. RESULTS

In Fig. 1(a), DLTS spectra of the as-received samples as well as samples annealed at 1250 °C for durations of 1.5, 2.5, and 6.6 h are shown. In the as-received state, peaks belonging to the donor freeze-out (at 50 K), the Ti_{Si} defect, and the V_C ($Z_{1/2}$ level) can be detected. The concentration of V_C amounts to 1.5×10^{11} cm^{-3}. After

Published under an exclusive license by AIP Publishing

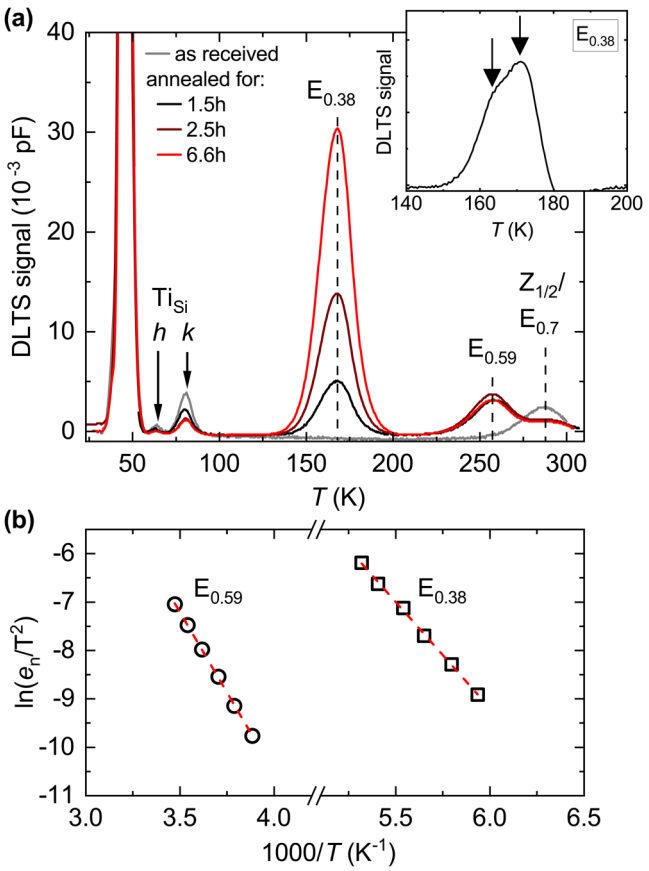

FIG. 1. (a) Complete DLTS spectra [rate window (640ms)$^{-1}$] of the as received as well as samples annealed for different durations. Inset: DLTS spectrum of the $E_{0.38}$ trap with a high-resolution weighting function obtained on the 2.5 h annealed sample, revealing two components of the level. (b) Plot of the reduced emission rates of the $E_{0.38}$ and $E_{0.59}$ traps and respective Arrhenius fits.

annealing under the C-rich environment of the C-cap, several observations can be made. Most prominently, two new traps appear at temperatures of about 170 (labeled $E_{0.38}$) and 265 K (labeled $E_{0.59}$), respectively. Their activation energies and apparent electron capture cross sections, determined from the reduced emission rate data in Fig. 1(b), are given in Table I. Note that the activation energy and apparent electron capture cross section for the 170 K peak are similar to the values previously found on the M_1 level ($E_a = 0.42$eV, $\sigma_n = 6 \times 10^{-15}$cm^2).[17] Given the fact that the M center has previously been shown to originate from charge transition levels (CTLs) of the C_i,[24] and taking into account that during the present experiment, considerable amounts of carbon can be expected to be continuously driven into the uppermost regions of the epilayer, which suggests the presence of the C_i defect, it is tempting to identify the trap emitting at 170 K with the M_1 level. However, the data presented in the further course of this paper casts doubt on this identification; therefore, we choose to adhere to the temporary label $E_{0.38}$ within this work. Note that while the amplitude of $E_{0.38}$ increases with annealing time, the amplitude of the $E_{0.59}$ level is approximately the same for all annealed samples, suggesting a different microscopic origin of the defects behind the two signatures. Although the activation energy of $E_{0.59}$ matches the one found experimentally for the M_2 level (0.63 eV[24]), it seems unlikely that they are identical, given their different peak emission temperatures (265 K for $E_{0.59}$ vs typically 295 K for M_2).

TABLE I. Experimentally determined properties (activation energy E_a, apparent electron capture cross section σ_n, app, and peak temperature T) of the $E_{0.38}$, $E_{0.59}$, and $E_{0.7}$ traps.

Trap label	E_a (eV)	σ_n, app (cm^2)	T (K)
$E_{0.38}$	0.38	5×10^{-15}	170
$E_{0.59}$	0.59	2×10^{-14}	265
$E_{0.7}$	0.7	4×10^{-13}	295

A second important observation from Fig. 1(a) is that the concentration of the $Z_{1/2}$ level, originating from the (0/2 −) CTL of the V_C defect, is apparently reduced from an initial value of 3×10^{11} cm^{-3} (corresponds to a V_C concentration of 1.5×10^{11} cm^{-3}) by roughly a factor of 2 for an annealing time of 1.5 h and stays approximately constant for longer annealing. Because it is located on the decreasing flank of the $E_{0.59}$ peak and also occurs nearly outside of the accessible temperature range, the activation energy of the shoulder appearing on the annealed samples can only be estimated by simulations of the DLTS spectra, assuming certain values for E_a and σ_n. According to such simulations, E_a amounts to roughly 0.7 eV and is, therefore, similar to that of $Z_{1/2}$ ($E_a = 0.67$eV). However, the depth profile for this level, which is presented further below, is incompatible with that expected for $Z_{1/2}$. We, therefore, conclude that this level does not originate from V_C but from a different point defect. In the further course of this paper, this level will be labeled $E_{0.7}$ based on its approximate activation energy. We note that the reduction of [$Z_{1/2}$] (and, therefore, [V_C]) to below the detection limit of DLTS by the presented annealing procedure is striking and supports the claim of carbon being injected into the epilayer, leading to C_i and V_C recombining.

A characteristic behavior of the M center is its bistability with respect to annealing at moderate temperatures (up to 200 °C) with and without applied bias.[18,37,38] Specifically, an annealing at zero bias and $T = 450$K leads to the reduction of the M_1 (and M_3 that lies outside of the studied range) amplitude and the emergence of the M_2 level; annealing at 310 K with a large reverse bias will restore the original DLTS spectrum without loss of the M_1 and M_3 amplitudes. The specified annealing procedures (reverse bias annealing at $V = -20$V for 20 min; zero-bias anneals at 0 V for 20 min) have been performed on the 2.5 h-annealed sample, the results of which are shown in Fig. 2. As can be seen in the figure, the $E_{0.38}$ amplitude is reduced to below the detectivity limit ($< 5 \times 10^{10}$cm^{-3}) by zero-bias annealing at 450 K; however, it remains undetectable after the reverse annealing step. Based on the formation energies for C_i-related defects published in Ref. 24, it can be calculated that the chosen bias annealing conditions would lead to a conversion of the M center between its two configurations

Published under an exclusive license by AIP Publishing

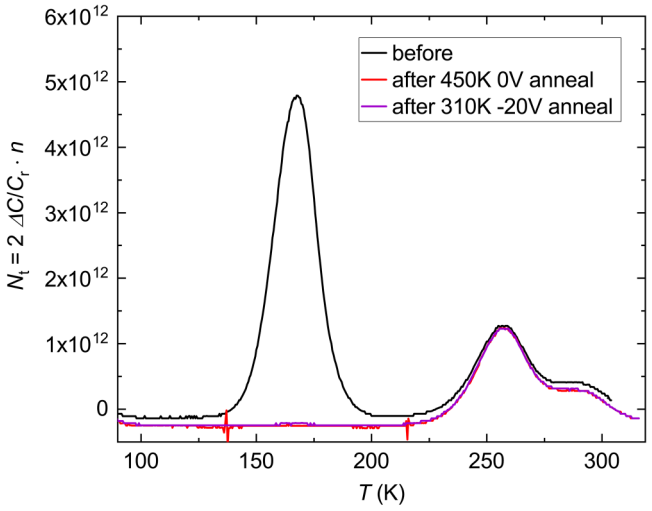

FIG. 2. Bias annealing behavior of the defect signatures detected by DLTS upon C injection, collected on the 2.5 h-annealed sample.

in a range between 2.1 and 9.5 μm into the epilayer. This range coincides almost entirely with the probing depth of the $E_{0.38}$ level; therefore, the conversion should be detectable. The absence of a recovery of the original signal intensity is, therefore, incompatible with $E_{0.38}$ being identical to M_1. Moreover, the amplitudes of $E_{0.59}$ and $E_{0.7}$ remain unaffected by the annealing procedure, supporting the hypothesis that they originate from another point defect—one

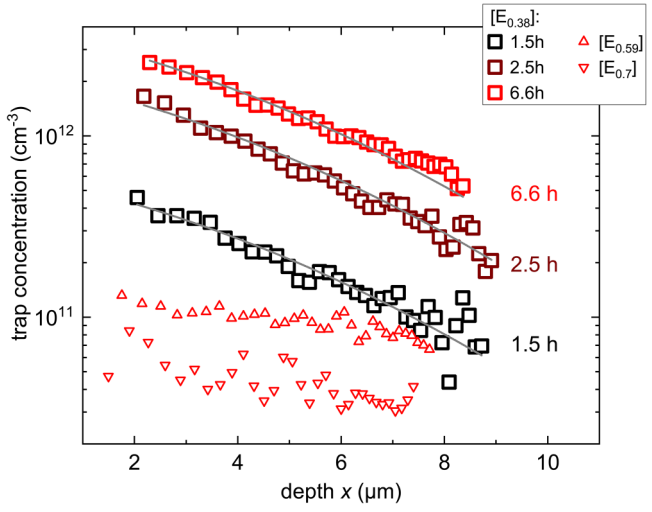

FIG. 3. Concentration profiles of the $E_{0.38}$, $E_{0.59}$, and $E_{0.7}$ levels, determined by DLTS profiling. Profiles of [$E_{0.38}$] are shown for all annealing times. Profiles of [$E_{0.59}$] and [$E_{0.7}$] are shown only for the 6.6 h anneal. Fits to the $E_{0.38}$ profiles according to Eq. (1) are shown in gray.

TABLE II. Diffusion parameters of the $E_{0.38}$ trap, determined from DLTS depth profiles in Fig. 3: diffusion constant D, surface concentration c_0, and an estimate of the value of the injection barrier E_i.

t_{ann} (h)	D (cm^2 s^{-1})	c_0 (cm^{-3})	E_i (eV)
1.5		1.2×10^{12}	
2.5		4.6×10^{12}	
6.6		7.3×10^{12}	
(Coupled)	6.03×10^{-12}		2.5–2.8

that is more stable than $E_{0.38}$. Importantly, they are likewise unrelated to the M center.

Concentration vs depth profiles for the traps $E_{0.38}$, $E_{0.59}$, and $E_{0.7}$ were recorded by varying the voltage pulse height, from $V_p = 0.5$ to 20 V, using a reverse bias of −20 V, and at a fixed temperature. The λ correction was taken into account. The resulting trap concentration profiles are displayed in Fig. 3. For $E_{0.38}$, a clear increase in concentration toward shallower depths is seen, in compliance with a defect entering the epilayer from the surface. For the $E_{0.59}$ and $E_{0.7}$ levels, the signal amplitude is lower than for $E_{0.38}$; however, a slight decrease toward the sample bulk can be observed here as well. The $E_{0.38}$ concentration profiles have been fitted with the relation

$$c(x) = \frac{c_0}{2} \cdot \mathrm{erfc}\left\{\frac{x}{2\sqrt{D t_{ann}}}\right\}, \quad (1)$$

where c_0 is the concentration of $E_{0.38}$ at $x = 0$, D is the diffusion constant, and t_{ann} the annealing time. From these fits to the concentration profiles obtained from DLTS for $t = 1.5$, 2.5, and 6.6 h, D and c_0 were determined and are given in Table II. Note that because the experiment was conducted at the same temperature for the different t_{ann}, the diffusion constant D should be identical across the three samples (assuming that no transient effects occur); therefore, the value of D was coupled between the datasets during fitting. The diffusion is expected to be thermally activated according to

$$D(T) = D_0 \exp\left\{-\frac{E_i}{k_B T}\right\}, \quad (2)$$

with D_0 being the pre-exponential factor, usually $D_0 \approx 10^{-2}$–10^{-3} cm^2 s^{-1} for atomic hops, and E_i being the injection barrier. An estimate of E_i can be given based on Eq. (2), and the values are also given in Table II. It must be noted that the method used here to extract an activation energy for the trap injection and diffusion is not very accurate since only one annealing temperature was used. In particular, this method relies on an assumed value of D_0, which may differ from the real value and which can only be determined by an experiment where varying temperatures are used. However, even for the range of D_0 values given above, the resulting range of the estimated activation energy amounts to 2.5–2.8 eV and, in effect, can still be considered small compared to migration barriers associated with diffusion of certain defect species, such as V_C.[39] Importantly, the determined value range for E_i is in accordance with those predicted by DFT for the diffusion of the neutrally charged C_i defect

Published under an exclusive license by AIP Publishing

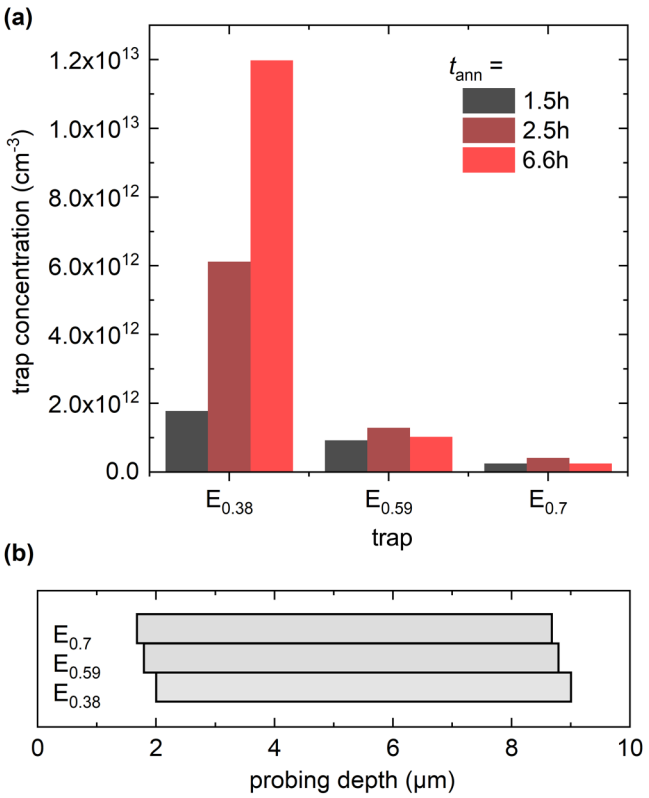

FIG. 4. (a) Concentrations of all four traps induced by annealing with C-cap in dependence on annealing time and (b) the probing depth of the three traps for the DLTS measurement conditions used in the experiment.

along the *c* axis of 4*H*-SiC ($E_{m,th} = 2.20$eV).[24] We, therefore, refer to the injection barrier for $E_{0.38}$ as the migration barrier for C_i for the remainder of this paper, although it is possible that an additional barrier for release from the C-cap is incorporated in this value.

The depth profiles of $E_{0.59}$ and $E_{0.7}$ appear to be flatter than that of $E_{0.38}$ but retain a slight downward slope toward the sample bulk. The low concentrations and high noise levels prevent a reliable extraction of formation barriers for the two deeper levels (the detection limit for defects under the conditions of the experiment is approximately $5 \times 10^{10}\,\mathrm{cm}^{-3}$). We observe that although $E_{0.59}$ and $E_{0.7}$ also appear to be coming in from the surface, they are likely of a different origin than $E_{0.38}$. Importantly, the depth profiles in Fig. 3 emphasize that the $E_{0.7}$ level is likely unrelated to V_C because in that case, as was noted further above, its concentration should decrease toward the surface as a result of the C injection.

IV. DISCUSSION

In Fig. 4, the evolution of the concentrations of the three annealing-induced traps is shown for varying t_{ann}. It can be seen that while $[E_{0.38}]$ clearly increases with longer anneals, $[E_{0.59}]$ and $[E_{0.7}]$ do not seem to show such a systematic behavior. It, therefore, appears that, while all three traps are formed by C injection, they originate from microscopically different defects. This is also supported by their different annealing behavior (see Fig. 2). As stated already, the injection barrier for the $E_{0.38}$ level matches well with the predicted value for C_i migration, and its activation energy of 0.38 eV is close to that of the M_1 level, which has previously been tied to the $(-/2-)$ acceptor level of C_i.[24,38] However, the M center possesses four charge transition levels in total, labeled M_1–M_4. They appear in pairs (M_1 and M_3, M_2 and M_4), which are now believed to belong to two configurations of the carbon split interstitial that can be reversibly converted into each other. $M_{1,2}$ are thought to originate from the $(-/2-)$ CTL, while $M_{3,4}$ stem from the deeper-lying $(0/-)$ CTL. Depending on the orientation of the C–C dimer, one of the two level pairs becomes dominant over the other, and because the conversion between them is connected to barriers <2eV, it can be triggered repeatedly by bias annealing procedures close to room temperature. In the experiments for the present paper, however, there were no further signatures resembling those of the M center apart from $E_{0.38}$ that matches M_1; DLTS scans up to 360 K revealed no further peaks being present. Taking into account the lack of the reversible character of the bias annealing of the observed defect signatures, as reported for the M center, we, therefore, suggest that the $E_{0.38}$ level is different from M_1, although it is most likely also related to the C_i defect.

$E_{0.59}$ and $E_{0.7}$ do not exhibit a monotonous variation of their concentration with C injection time; however, their occurrence only after the annealing experiment and the possible slight increase of their concentration profile toward the sample's surface (see Fig. 3) suggest that they originate from a defect that has been driven into the SiC epilayer during the anneals. Okuda *et al.* have reported that the thermal oxidation of 4*H*-SiC followed by an anneal in Ar atmosphere at 1550 °C leads to the formation of a pair of electron traps labeled ON0a and ON0b.[40] The authors propose that ON0a is identical to the EO1 minority trap found in *p*-type material after thermal oxidation; hence, a correlation with carbon injection is conceivable. ON0a and EO1 possess the same energy with respect to the conduction band edge ($E_t = E_C - 0.59$eV), which also coincides with the activation energy of the $E_{0.59}$ trap found in this work. Okuda *et al.* do not report the activation energy of ON0b; however, its maximum emission occurs at a temperature roughly 30 K higher than for ON0a, which is the same temperature difference as between the $E_{0.59}$ and $E_{0.7}$ traps in the present work. It seems, therefore, likely that the $E_{0.59}$ and $E_{0.7}$ levels are the same as those labeled ON0a and ON0b by Okuda *et al.*, respectively. Furthermore, the EO1 minority trap has been tentatively attributed to the carbon split di-interstitial $(C_{sp})_2$ by Okuda *et al.* based on *ab initio* calculations by Bockstedte *et al.*[41] Specifically, the latter authors calculated the $(0/2-)$ CTLs of the *hh* and *kk* configurations of that defect, which is predicted to show negative-*U* properties, to be situated around 0.55 and 0.63 eV below the conduction band minimum, respectively, which roughly matches the measured activation energies for $E_{0.59}$ and $E_{0.7}$. Bockstedte *et al.* also calculate the C split di-interstitial to be particularly stable: its predicted dissociation energy amounts to 4.6 eV in both *hh* and *kk* configurations, in accordance with the observed temperature stability of $E_{0.59}$ and $E_{0.7}$ as compared to that of $E_{0.38}$. An interesting question is how the defect behind $E_{0.38}$ can form at

Published under an exclusive license by AIP Publishing

temperatures as high as 1250 °C, as well as survive during the cool-down ramp to room temperature (about 6 h in total) but anneal out at only 450 K during the bias anneals. A possible explanation is that the presence of the built-in electric field of the Schottky barrier promotes the diffusion of C_i out of the depletion region. Furthermore, the migration or injection barrier of 2.5–2.8 eV determined from the depth profile of $E_{0.38}$ only reflects the high-temperature conditions present during the carbon injection, which promote a midgap Fermi level. These typically induce more positive charge states on point defects for which migration barriers are typically higher than when the defect is negatively charged.

Unfortunately, the authors of Ref. 41 did not calculate CTLs of the single C_i in 4*H*-SiC to compare with those of di-interstitials. Kobayashi *et al.* have used hybrid-functional DFT calculations to predict the formation energies and CTLs of various native point defects and clusters in 4*H*-SiC.[22] They find the $(0/-)$ CTL of the carbon split mono-interstitial $C_{i,split}$ in its *k* and *h* configurations at E_C 0.7 and 0.33 eV, respectively. While the latter is a reasonably good match for $E_{0.38}$ and the former for $E_{0.7}$, the different injection and annealing behavior for the two traps found in this work contradict a common microscopic origin. Kobayashi *et al.* also discuss the case of carbon clusters to a limited extent and claim that according to their calculations, poly-interstitials exhibit too high formation energies to be stable. Alternatively, they find the di-carbon antisites $(C_2)_{Si}$ to be highly stable and to have their $(0/-)$ CTLs at $E_C - 0.5$eV (*k*) and $E_C - 0.13$eV (*h*). Again, while the former approximately matches the activation energy of $E_{0.59}$, the latter does not seem to have a corresponding trap found in our data [apart from the unequivocally identified $Ti_{Si}(h)$ level].

It is interesting to note that even though the surface of the epilayer had been partly oxidized during the annealing because of the dissolving carbon cap, the traps that have been observed here are typically not produced in oxidation experiments (with the exception, perhaps, of ON0 in Ref. 40)—compare, e.g., to Ref. 42 where no emission from defects is detected between 100 and 350 K. This observation indicates that oxygen is not involved in the formation of the defects behind the three levels observed in the present study. The oxidation in this work has only led to a very thin oxide layer in which case only few interstitial-related defects are released into the epilayer[43] such that the dominant source of interstitial atoms can be expected to be the carbon cap. While Si injection can, in theory, occur during oxidation experiments,[43,44] the formation energy of Si_i has been calculated to be high compared to that of C_i under *n*-type conditions[24,45] such that $[C_i] \gg [Si_i]$ can be expected. Therefore, an Si-related origin of the traps formed in the present experiments can likely be excluded.

Overall, it is challenging to make assignments of the observed trap signatures to specific point defects at this point. However, it can be noted that carbon injection, in the near absence of V_C, leads to the formation of several new defect levels related to C excess and that there are at least two physically differing defect structures involved: a less stable one, increasing in concentration as more carbon is injected, possibly hinting at a mono-interstitial as its microscopic origin, and a more stable one that seems to possess a more complicated formation and annealing behavior, which may be due to a larger carbon complex. Annihilation of V_C by carbon injection, therefore, seems to be a rather complicated process. One plausible scenario is that this involves the migration of C in the form of single interstitials C_i, which, in the further course of the injection and migration process, form higher-order, more stable complexes. The absence of the M center in this work demonstrates that excess carbon forms a larger variety of interstitial-related defects than previously thought.

V. CONCLUSION

Using a carbon cap on the surface of *n*-type 4*H*-SiC epilayers, we have injected excess carbon by thermal annealing. Because the initial concentrations of carbon vacancies V_C were low, the C injection leads to (1) complete annihilation of V_C and (2) the formation of new C excess-related defects. A set of three defect levels becomes visible in low-temperature DLTS spectra, with activation energies of 0.38, 0.59, and 0.7 eV. Depth profiles of the trap levels show that they originate from C injection (the defect concentration increases toward the epilayer surface), and the activation energy associated with the evolution of the depth profiles matches the migration energy for carbon diffusion previously calculated by *ab initio* methods. The dissimilar behavior of the traps with longer injection duration as well as their starkly differing thermal stability point toward different defect structures behind the signatures, albeit likely related to carbon interstitials in all cases. An identification of either of the defects with the M center, which has previously been attributed to the mono-interstitial C_i, does not appear justified. However, the ON0a and ON0b defects found in thermally oxidized material, and possibly originating from the carbon split di-interstitial $(C_{sp})_2$, match the levels at E_C of 0.59 and 0.7 eV well. Generally, this work emphasizes the complexity of the V_C annihilation process via supply of excess carbon, which seems to take place through a variety of channels.

ACKNOWLEDGMENTS

Financial support was kindly provided by the Research Council of Norway and the University of Oslo through the frontier research project FUNDAMeNT (No. 251131, FriPro ToppForsk program). The Research Council of Norway is acknowledged for the support to the Norwegian Micro- and Nano-Fabrication Facility, NorFab (Project No. 295864). The work of M.E.B. was supported by an ETH Zurich Postdoctoral Fellowship.

AUTHOR DECLARATIONS

Conflict of Interest

The authors have no conflict of interest to declare.

DATA AVAILABILITY

The data that support the findings of this study are available from the corresponding author upon reasonable request.

REFERENCES

[1]M. Widmann, S.-Y. Lee, T. Rendler, N. T. Son, H. Fedder, S. Paik, L.-P. Yang, N. Zhao, S. Yang, I. Booker, A. Denisenko, M. Jamali, S. A. Momenzadeh, I. Gerhardt, T. Ohshima, A. Gali, E. Janzén, and J. Wrachtrup, "Coherent control

Published under an exclusive license by AIP Publishing

of single spins in silicon carbide at room temperature," Nat. Mater. **14**, 164–168 (2014).
[2]S. Castelletto, B. C. Johnson, V. Ivády, N. Stavrias, T. Umeda, A. Gali, and T. Ohshima, "A silicon carbide room-temperature single-photon source," Nat. Mater. **13**, 151–156 (2014).
[3]D. J. Christle, A. L. Falk, P. Andrich, P. V. Klimov, J. Ul Hassan, N. T. Son, E. Janzén, T. Ohshima, and D. D. Awschalom, "Isolated electron spins in silicon carbide with millisecond coherence times," Nat. Mater. **14**, 160–163 (2015).
[4]H. J. von Bardeleben, J. L. Cantin, A. Csóré, A. Gali, E. Rauls, and U. Gerstmann, "NV centers in 3C, 4H, and 6H silicon carbide: A variable platform for solid-state qubits and nanosensors," Phys. Rev. B **94**, 121202 (2016).
[5]K. Danno, D. Nakamura, and T. Kimoto, "Investigation of carrier lifetime in 4H-SiC epilayers and lifetime control by electron irradiation," Appl. Phys. Lett. **90**, 202109 (2007).
[6]N. T. Son, X. T. Trinh, L. S. Løvlie, B. G. Svensson, K. Kawahara, J. Suda, T. Kimoto, T. Umeda, J. Isoya, T. Makino, T. Ohshima, and E. Janzén, "Negative-U system of carbon vacancy in 4H-SiC," Phys. Rev. Lett. **109**, 187603 (2012).
[7]I. D. Booker, E. Janzén, N. T. Son, J. Ul Hassan, P. Stenberg, and E. A. Sveinbjörnsson, "Donor and double-donor transitions of the carbon vacancy related $EH_6/7$ deep level in 4H-SiC," J. Appl. Phys. **119**, 235703 (2016).
[8]L. Storasta, J. P. Bergman, E. Janzén, A. Henry, and J. Lu, "Deep levels created by low energy electron irradiation in 4H-SiC," J. Appl. Phys. **96**, 4909–4915 (2004).
[9]F. C. Beyer, C. G. Hemmingsson, H. Pedersen, A. Henry, J. Isoya, N. Morishita, T. Ohshima, and E. Janzén, "Capacitance transient study of a bistable deep level in e^--irradiated n-type 4H-SiC," J. Phys. D: Appl. Phys. **45**, 455301 (2012).
[10]R. M. Karsthof, M. E. Bathen, A. Galeckas, and L. Vines, "Conversion pathways of primary defects by annealing in proton-irradiated *n*-type 4H-SiC," Phys. Rev. B **102**, 184111 (2020).
[11]M. L. David, G. Alfieri, E. M. Monakhov, A. Hallén, C. Blanchard, B. G. Svensson, and J. F. Barbot, "Electrically active defects in irradiated 4H-SiC," J. Appl. Phys. **95**, 4728–4733 (2004).
[12]M. E. Bathen, A. Galeckas, J. Müting, H. M. Ayedh, U. Grossner, J. Coutinho, Y. K. Frodason, and L. Vines, "Electrical charge state identification and control for the silicon vacancy in 4H-SiC," npj Quantum Inf. **5**, 111 (2019).
[13]C. Hemmingsson, N. T. Son, O. Kordina, J. P. Bergman, E. Janzén, J. L. Lindström, S. Savage, and N. Nordell, "Deep level defects in electron-irradiated 4H-SiC epitaxial layers," J. Appl. Phys. **81**, 6155–6159 (1997).
[14]G. Alfieri and A. Mihaila, "Isothermal annealing study of the EH1 and EH3 levels in n-type 4H-SiC," J. Phys.: Condens. Matter **32**, 465703 (2020).
[15]H. K. Nielsen, D. Martin, P. Lévêque, A. Hallén, and B. Svensson, "Annealing study of a bistable defect in proton-implanted n-type 4H-SiC," Physica B **340-342**, 743–747 (2003).
[16]D. M. Martin, H. K. Nielsen, P. Lévêque, A. Hallén, G. Alfieri, and B. G. Svensson, "Bistable defect in mega-electron-volt proton implanted 4H silicon carbide," Appl. Phys. Lett. **84**, 1704–1706 (2004).
[17]H. K. Nielsen, A. Hallén, and B. G. Svensson, "Capacitance transient study of the metastable M center in n-type 4H-SiC," Phys. Rev. B **72**, 085208 (2005).
[18]H. K. Nielsen, A. Hallén, D. Martin, and B. G. Svensson, "M-center in low-dose proton implanted 4H-SiC; bistability and change in emission rate," Mater. Sci. Forum **483–485**, 497–500 (2005).
[19]J.-F. Wang, Q. Li, F.-F. Yan, H. Liu, G.-P. Guo, W.-P. Zhang, X. Zhou, L.-P. Guo, Z.-H. Lin, J.-M. Cui, X.-Y. Xu, J.-S. Xu, C.-F. Li, and G.-C. Guo, "On-demand generation of single silicon vacancy defects in silicon carbide," ACS Photonics **6**, 1736–1743 (2019).
[20]M. Bockstedte, A. Mattausch, and O. Pankratov, "*Ab initio* study of the migration of intrinsic defects in 3C-SiC," Phys. Rev. B **68**, 205201 (2003).
[21]A. Gali, P. Deák, P. Ordejón, N. T. Son, E. Janzén, and W. J. Choyke, "Aggregation of carbon interstitials in silicon carbide: A theoretical study," Phys. Rev. B **68**, 125201 (2003).
[22]T. Kobayashi, K. Harada, Y. Kumagai, F. Oba, and Y. ichiro Matsushita, "Native point defects and carbon clusters in 4H-SiC: A hybrid functional study," J. Appl. Phys. **125**, 125701 (2019).
[23]G. Alfieri, E. V. Monakhov, B. G. Svensson, and A. Hallén, "Defect energy levels in hydrogen-implanted and electron-irradiated n-type 4H silicon carbide," J. Appl. Phys. **98**, 113524 (2005).
[24]J. Coutinho, J. D. Gouveia, T. Makino, T. Ohshima, Ž. Pastuović, L. Bakrač, T. Brodar, and I. Capan, "M center in 4H-SiC is a carbon self-interstitial," Phys. Rev. B **103**, L180102 (2021).
[25]B. Zippelius, J. Suda, and T. Kimoto, "High temperature annealing of n-type 4H-SiC: Impact on intrinsic defects and carrier lifetime," J. Appl. Phys. **111**, 033515 (2012).
[26]L. Storasta, H. Tsuchida, T. Miyazawa, and T. Ohshima, "Enhanced annealing of the $Z_1/2$ defect in 4H-SiC epilayers," J. Appl. Phys. **103**, 013705 (2008).
[27]T. Hayashi, K. Asano, J. Suda, and T. Kimoto, "Enhancement and control of carrier lifetimes in p-type 4H-SiC epilayers," J. Appl. Phys. **112**, 064503 (2012).
[28]T. Miyazawa and H. Tsuchida, "Point defect reduction and carrier lifetime improvement of Si- and C-face 4H-SiC epilayers," J. Appl. Phys. **113**, 083714 (2013).
[29]H. M. Ayedh, A. Hallén, and B. G. Svensson, "Elimination of carbon vacancies in 4H-SiC epi-layers by near-surface ion implantation: Influence of the ion species," J. Appl. Phys. **118**, 175701 (2015).
[30]T. Hiyoshi and T. Kimoto, "Reduction of deep levels and improvement of carrier lifetime in n-type 4H-SiC by thermal oxidation," Appl. Phys. Express **2**, 041101 (2009).
[31]T. Hiyoshi and T. Kimoto, "Elimination of the major deep levels in n- and p-type 4H-SiC by two-step thermal treatment," Appl. Phys. Express **2**, 091101 (2009).
[32]H. M. Ayedh, R. Nipoti, A. Hallén, and B. G. Svensson, "Elimination of carbon vacancies in 4H-SiC employing thermodynamic equilibrium conditions at moderate temperatures," Appl. Phys. Lett. **107**, 252102 (2015).
[33]H. M. Ayedh, R. Nipoti, A. Hallén, and B. G. Svensson, "Thermodynamic equilibration of the carbon vacancy in 4H-SiC: A lifetime limiting defect," J. Appl. Phys. **122**, 025701 (2017).
[34]A. A. Istratov, "New correlation procedure for the improvement of resolution of deep level transient spectroscopy of semiconductors," J. Appl. Phys. **82**, 2965–2968 (1997).
[35]A. A. Istratov, O. F. Vyvenko, H. Hieslmair, and E. R. Weber, "Critical analysis of weighting functions for the deep level transient spectroscopy of semiconductors," Meas. Sci. Technol. **9**, 477–484 (1998).
[36]C. Zimmermann, Y. K. Frodason, V. Rønning, J. B. Varley, and L. Vines, "Combining steady-state photo-capacitance spectra with first-principles calculations: The case of Fe and Ti in β-Ga_2O_3," New J. Phys. **22**, 063033 (2020).
[37]F. C. Beyer, C. Hemmingsson, H. Pedersen, A. Henry, E. Janzén, J. Isoya, N. Morishita, and T. Ohshima, "Annealing behavior of the EB-centers and M-center in low-energy electron irradiated n-type 4H-SiC," J. Appl. Phys. **109**, 103703 (2011).
[38]I. Capan, T. Brodar, R. Bernat, Ž. Pastuović, T. Makino, T. Ohshima, J. D. Gouveia, and J. Coutinho, "M-center in 4H-SiC: Isothermal DLTS and first principles modeling studies," J. Appl. Phys. **130**, 125703 (2021).
[39]M. E. Bathen, H. M. Ayedh, L. Vines, I. Farkas, E. Janzén, and B. G. Svensson, "Diffusion of the carbon vacancy in a-cut and c-cut n-type 4H-SiC," Mater. Sci. Forum **924**, 200–203 (2018).
[40]T. Okuda, G. Alfieri, T. Kimoto, and J. Suda, "Oxidation-induced majority and minority carrier traps in n- and p-type 4H-SiC," Appl. Phys. Express **8**, 111301 (2015).
[41]M. Bockstedte, A. Mattausch, and O. Pankratov, "*Ab initio* study of the annealing of vacancies and interstitials in cubic SiC: Vacancy-interstitial recombination and aggregation of carbon interstitials," Phys. Rev. B **69**, 235202 (2004).
[42]K. Kawahara, J. Suda, and T. Kimoto, "Deep levels generated by thermal oxidation in n-type 4H-SiC," Appl. Phys. Express **6**, 051301 (2013).
[43]D. Goto and Y. Hijikata, "Unified theory of silicon carbide oxidation based on the Si and C emission model," J. Phys. D: Appl. Phys. **49**, 225103 (2016).
[44]Y. Hijikata, H. Yaguchi, and S. Yoshida, "Theoretical studies for Si and C emission into SiC layer during oxidation," Mater. Sci. Forum **679–680**, 429–432 (2011).
[45]J. Coutinho, "Theory of the thermal stability of silicon vacancies and interstitials in 4H-SiC," Crystals **11**, 167 (2021).

Published under an exclusive license by AIP Publishing